Supplemental Figure S1.

Characteristics of *Lnk*$^{-/-}$ platelets.

(A) Electron micrographs of resting platelets showing the normal intracellular structure of *Lnk*$^{-/}$ platelets. Samples were fixed with 4% PFA in suspension and sectioned for observation. Bar, 1 μm.

(B) Comparable expression of major integrin subunits and glycoproteins on the surface of resting WT and *Lnk*$^{-/-}$ platelets.

Supplemental Figure S2.

Relationship between platelet counts and bleeding times in chimeric recipient mice post-transplantation.

(A) WT-and Lnk-chimeric recipients were randomly selected 2, 4, 6, and 8 wks post-transplantation to examine circulating platelet counts (X-axes) and tail bleeding and re-bleeding times (red squares or circles) (Y-axes). While most WT-chimeras that re-bled had platelet counts less than 5.5 x10^{8}/ml (8 of 10 mice that re-bred, total number = 34, left panel), 15 of 30 Lnk-chimeras rebred independently of the time post-transplantation and platelet counts (right panel). (B) Graph plotting platelet counts (X-axis) against 1/bleeding times (Y-axis). The relation suggests that Lnk-chimeras have a greater tendency to bleed independently of platelet counts than WT-chimeras. The black ($y = 0.000018x + 0.0047$) and gray lines ($y = 0.000041x + 0.0051$) were fitted to data from the Lnk-and WT-chimeras, respectively.

Supplemental Figure S3.

Time course of spreading in the absence of an agonist (A) and without granule secretion in the absence or presence of thrombin (B).

(A) Washed platelets from WT (WT) and *Lnk*$^{-/-}$ mice were plated on fibrinogen-coated 35-mm glass bottom dishes as in Figure 4A (no agonist). The upper panel depicts representative DIC images of WT and *Lnk*$^{-/-}$ platelets captured in real time at the indicated times. Surface areas of individual platelets were measured at various times using Image-J software (mean ± SD; n = 6 platelets from two independent experiments). (B) Experiments similar to those in Fig. 4A were done in the presence of apyrase and indomethacin to block granule secretion. Thrombin (0.05 U/ml)

induced apparent lamellipodial protrusion in adherent WT platelets (arrow heads) but not in *Lnk*$^{-/-}$ platelets. Right panel shows the mean platelet surface areas at 45 min (mean ± SD; n = 50). Bar, 10 μm.

Supplemental Figure S4.

***Lnk* deficiency does not affect integrin activation (inside-out signaling) or alpha-granule secretion in platelets**.

(A) Washed WT and *Lnk*$^{-/-}$ platelets were incubated for 30 min at room temperature with Alexa 488-fibrinogen in the presence of the indicated agonists, after which fibrinogen binding was quantified by flow cytometry. Data are means ± SD of five independent experiments. (B) Representative traces with histograms showing P-selectin expression in the presence of thrombin.

Supplement Figure S5.

The C-terminal portion of Lnk is indispensable for c-Src-mediated Lnk phosphorylation and stable lamellipodia formation.

(A) Flag-tagged WT Lnk (WT-Lnk) or a Lnk mutant lacking the C-terminal portion (ΔC-Lnk) were expressed in COS7 cells, with or without a constitutively active form of c-Src (CA-Src). Cells were lysed 48 hr after transfection, immunoprecipitated with anti-Flag Ab, and then subjected to immunoblotting using anti-pTyr. (B) CHO cells expressing human αIIbβ3 were transfected with GFP-tagged WT-Lnk or ΔC-Lnk in the absence or presence of Fyb. Co-expression of Fyb with WT-Lnk accelerated lamellipodia formation in CHO transfectants, as CHO cells do not express Fyb endogenously. CHO cells endogenously express c-Src and Fyn. The cells were incubated for 18 h in medium containing 10% FBS and then serum starved (0.5% FBS) for 12 h. The morphology of spreading platelets was observed after they had adhered to fibrinogen-coated cover glass in the presence of $CaCl_2$ and $MgCl_2$, but not $MnCl_2$, for 60 min. The cells were stained with rhodamine-phalloidin to label F-actin (red). Whereas WT-Lnk promoted lamellipodia formation (arrowheads, lamellipodia were observed in 62% of 50

cells) in transfectants, ΔC-Lnk transfectants showed less spreading and fewer lamellipodia, but prominent filopodia formation (arrows, lamellipodia were observed in 14% of 50 cells). Bar, 20 μm.

Supplement Figure S6.

***In vivo* thrombus formation is impaired in *Fyn*$^{-/-}$ mice.**

Single-shot images of mesenteric capillaries (A) and arterioles (B) were obtained using intravital fluorescence microscopy before and 20 s after laser-induced injury. FITC-dextran was injected to visualize cell dynamics, while hematoporphyrin was injected to produce ROS upon laser irradiation (1.8 mg/kg for capillary thrombi, 2.5 mg/kg for arterioles). Supplemental videos are available (*Fyn*$^{-/-}$ in *A* = video 5 and *Fyn*$^{-/-}$ in *B* = video 6). The numbers of platelets in developing thrombi after laser-induced injury in capillaries (A) and arterioles (B) were calculated. Y-axes represent the numbers of platelets per μm of observed vessel length. Open boxes denote WT, closed boxes *Fyn*$^{-/-}$; lines denote the median value for each group. The diameters of the vessels examined were comparable. Note the impaired thrombus formation in both *Fyn*$^{-/-}$ capillaries and arterioles, as compared to WT. Bar, 10 μm.

Supplementary Figure S7.

Vascular and endothelial integrity following laser-induced thrombus formation.

To assess damage to the vasculature and endothelial cell layer following laser-induced injury, we examined the vascular structure before (pre) and after (post) laser-induced injury in WT capillaries.
The vasculature was visualized by staining with Alexa-fluor-568-*Griffonia simplicifolia* IB_4 isolectin, which was known to specifically bind to endothelial cells (pseudo-colored in red). Whole blood cells were visualized using FITC-dextran (blue), and nuclei with Hoechst 33324 (green). This visualization revealed that the endothelium remained intact following laser-induced injury. Bar, 10 μm.

Video S1.

***In vivo* thrombus formation in a WT-chimera capillary**.

Thrombus formation was induced by laser injury in a mesenteric capillary in a WT-chimeric mice (8 wks post-transplantation, as shown in Fig. 3 A). First, platelets firmly adhere to the vessel wall. Second, platelets in the flowing blood acutely pile up, reducing the diameter of the vessel lumen and the blood flow velocity. Finally, the blood vessel is occluded by plugged erythrocytes and leukocytes (this final step is not shown in this video). The images were obtained at 30 frames/s using a 100x objective lens after injecting FITC-dextran and hematoporphyrin and were reconstructed at 3x-speed. All blood cells are visualized negatively. Note that the pulsating motion seen in the video is not from the heartbeat but is a combined motion artifact and includes respiratory movement. Bar, 10 μm.

Video S2.

***In vivo* thrombus formation in a Lnk-chimera capillary**.

Thrombus formation was induced by laser injury in a mesenteric capillary in Lnk-chimeric mice (4 wks post-transplantation, as shown in Fig. 3 A). Platelets in the blood flow adhere to the vessel wall in a manner similar to that seen in WT-chimeric mice. However, the adhesion is less firm and the number of platelets that pile up is smaller than in WT mice. In addition, part of the fragile aggregated platelet is washed out by the blood flow, and the remaining thrombus is even smaller. The images were obtained at 30 frames/s and reconstructed at 3x-speed. Bar, 10 μm.

Video S3.

***In vivo* thrombus formation in a WT capillary**.

Thrombus formation was induced by laser injury in a mesenteric WT (depicted as $Lnk^{+/+}$) capillary. First, platelets firmly adhere to the vessel wall. Second, platelets from the flowing blood acutely pile up, reducing the vessel lumen diameter and the blood flow velocity. Finally, the blood vessel is occluded (this final step not shown in this video).

The images were obtained at 30 frames/s using a 100x objective lens after injecting FITC-dextran and hematoporphyrin and reconstructed at 3x-speed. Blood cells were visualized negatively. Bar, 10 μm.

Video S4.

***In vivo* thrombus formation in a *Lnk*$^{-/-}$ capillary.**

Thrombus formation was induced by laser injury in a mesenteric *Lnk*$^{-/-}$ capillary. Platelets in the flowing blood adhere to the vessel wall in a manner similar that seen in *Lnk*$^{+/+}$ mice. However, the adhesion is looser than in WT mice, and the number of platelets that pile up is smaller. In addition, part of the fragile platelet aggregate is washed out by the blood flow, so that the resultant thrombus is even smaller. The images were obtained at 30 frames/s and reconstructed at 3x-speed. Bar, 10 μm.

Video S5.

***In vivo* thrombus formation in a WT arteriole**.

Thrombus formation was induced by laser injury in a mesenteric WT (depicted as *Lnk*$^{+/+}$) arteriole. The developing thrombus can be seen on the vascular wall. The images were reconstructed at 2x-speed. Bar, 10 μm.

Video S6.

***In vivo* thrombus formation in a *Lnk*$^{-/-}$ arteriole.**

Thrombus formation was induced by laser injury in a mesenteric *Lnk*$^{-/-}$ arteriole. The developing thrombus, which can be seen on the vascular wall, is smaller than those seen in WT mice (Video S5). The images were reconstructed at 2x-speed. Bar, 10 μm.

Video S7.

***In vivo* thrombus formation in a *Fyn*$^{-/-}$ capillary.**

Thrombus formation was induced by laser injury in a mesenteric *Fyn*$^{-/-}$ capillary. As in *Lnk*$^{-/-}$ mice, platelets

temporally adhere to the endothelium, but their adhesion is very fragile, and the number of platelets that pile up is markedly smaller than in WT mice (Video S3). Consequently, and the resultant thrombus is smaller. The images were reconstructed at 3x-speed. Bar, 10 μm.

Video S8.

***In vivo* thrombus formation in a *Fyn*$^{-/-}$ arteriole.**

Thrombus formation was induced by laser injury in a mesenteric *Lnk*$^{-/-}$ arteriole. The developing thrombus, which can be seen on the vascular wall, is smaller than those seen in WT mice (Video S4). The images were reconstructed at 2x-speed. Bar, 10 μm.

Takizawa, Nishimura et al. Figure S1

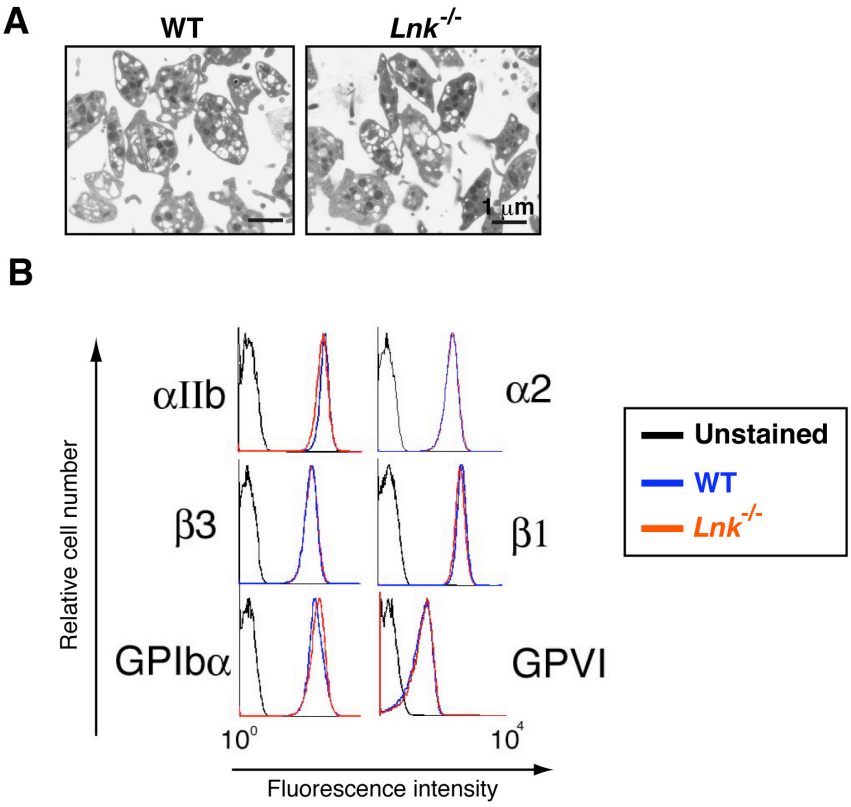

Takizawa, Nishimura et al. Figure S2

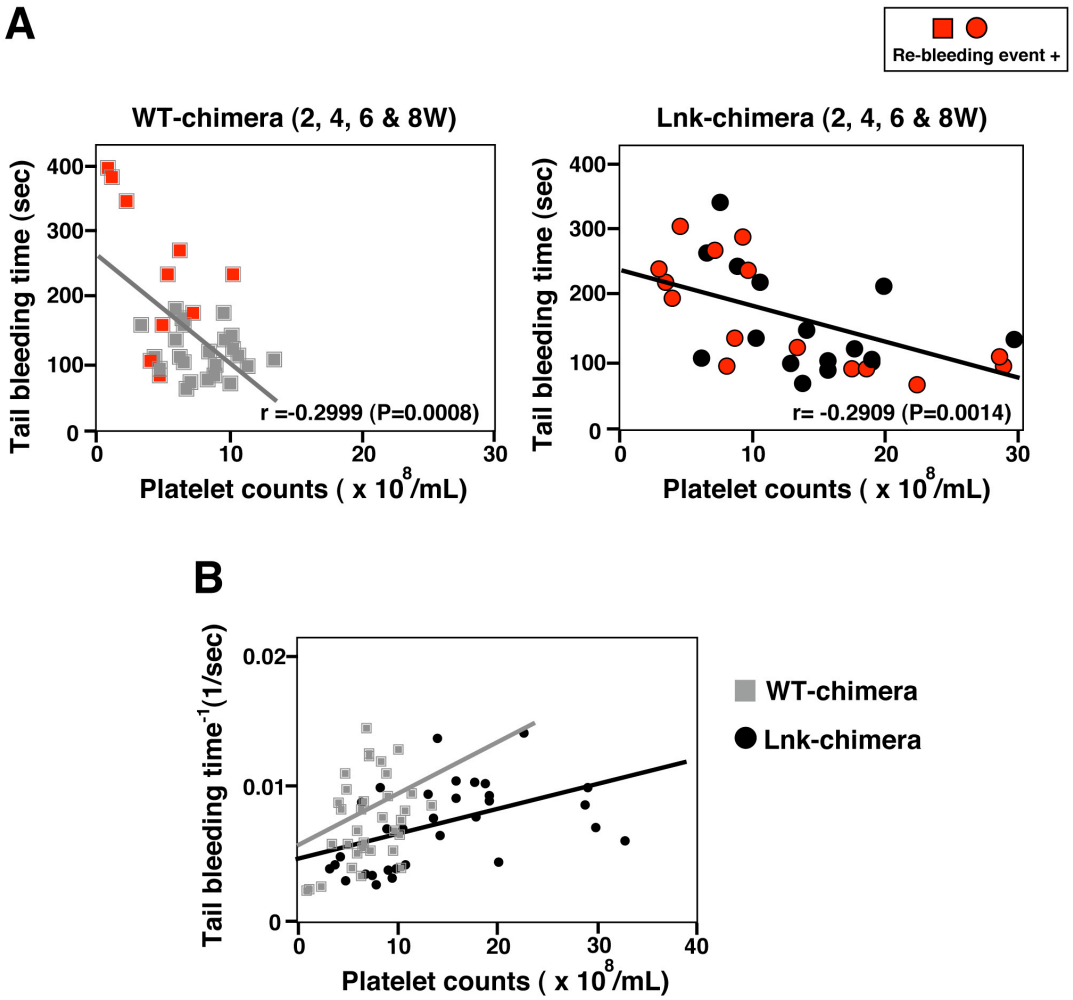

Takizawa, Nishimura et al. Figure S3

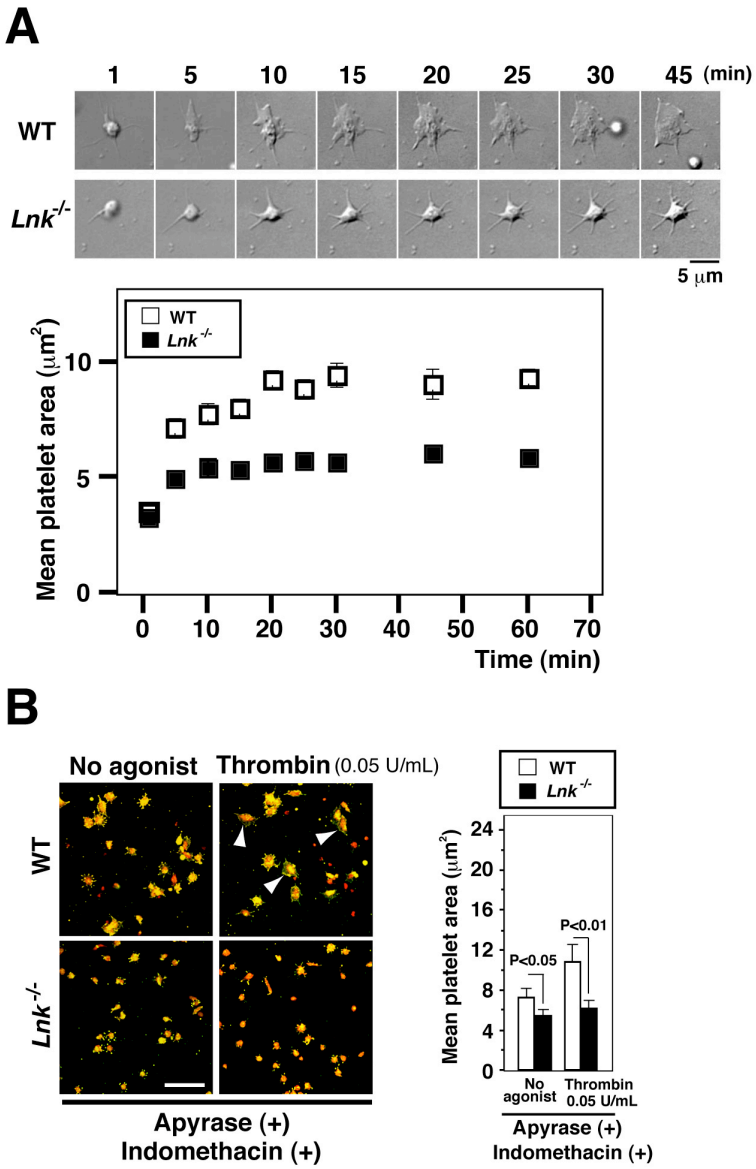

Takizawa, Nishimura et al. Figure S4

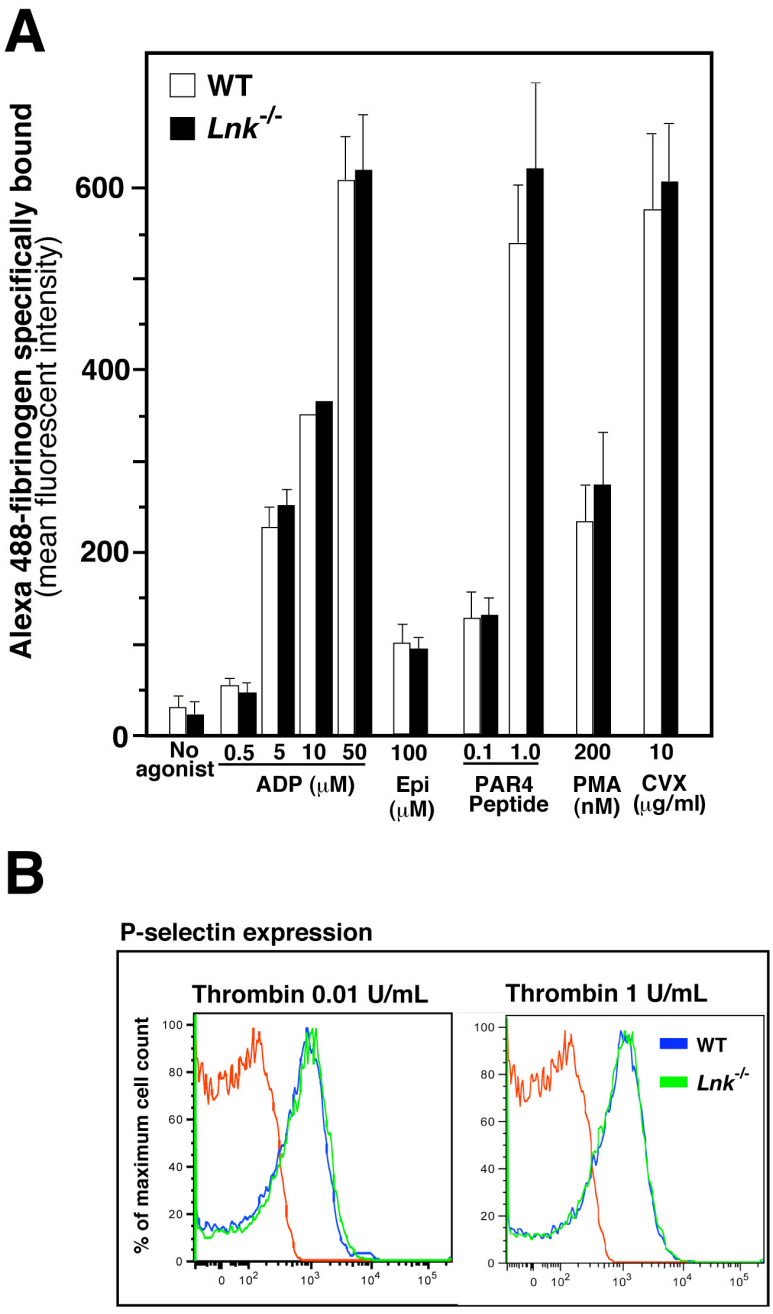

Takizawa, Nishimura et al. Figure S5

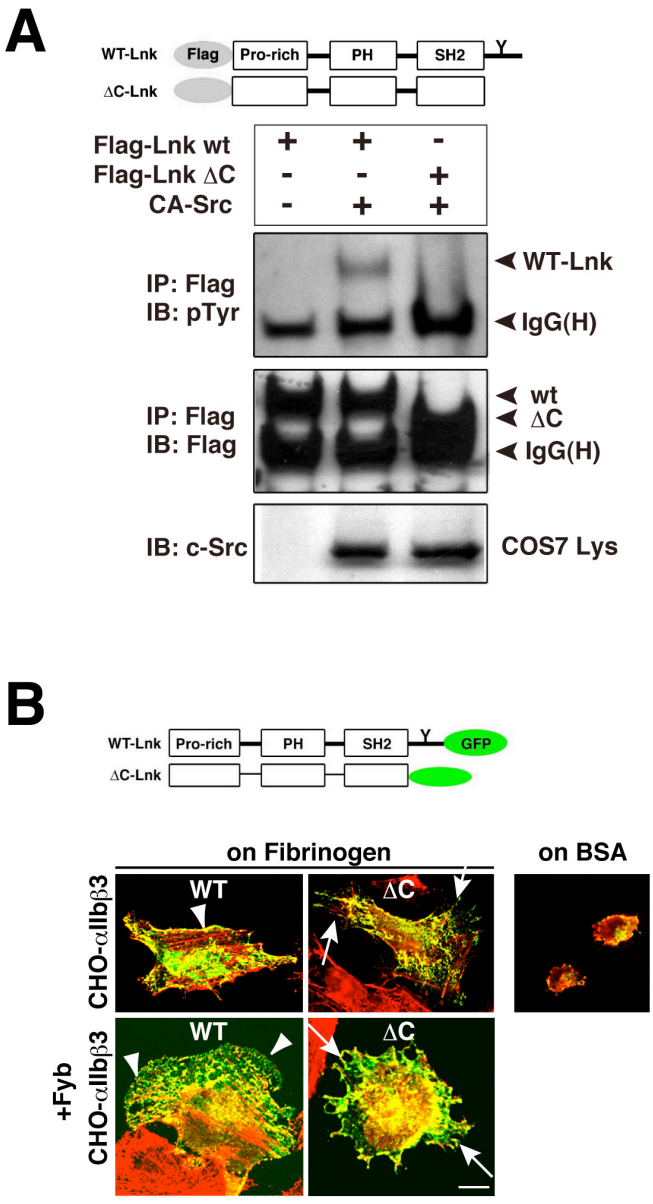

Takizawa, Nishimura et al. Figure S6

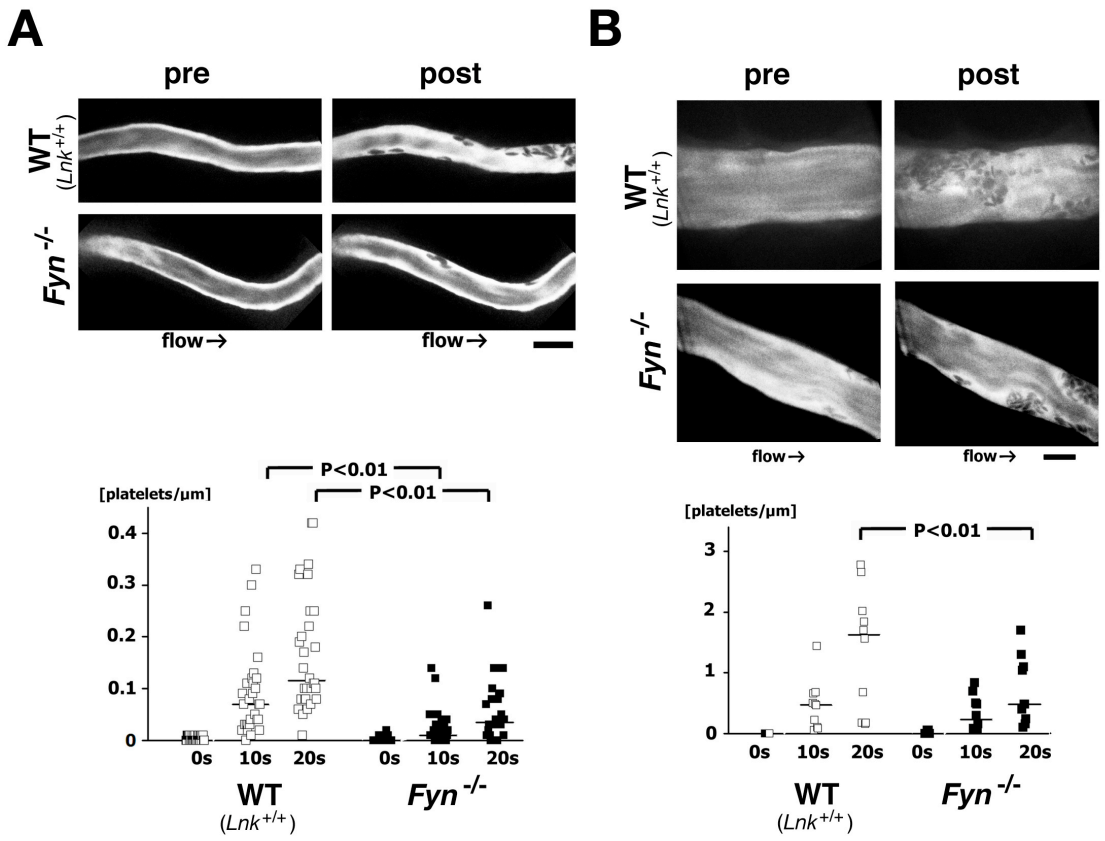

Takizawa, Nishimura et al. Figure S7

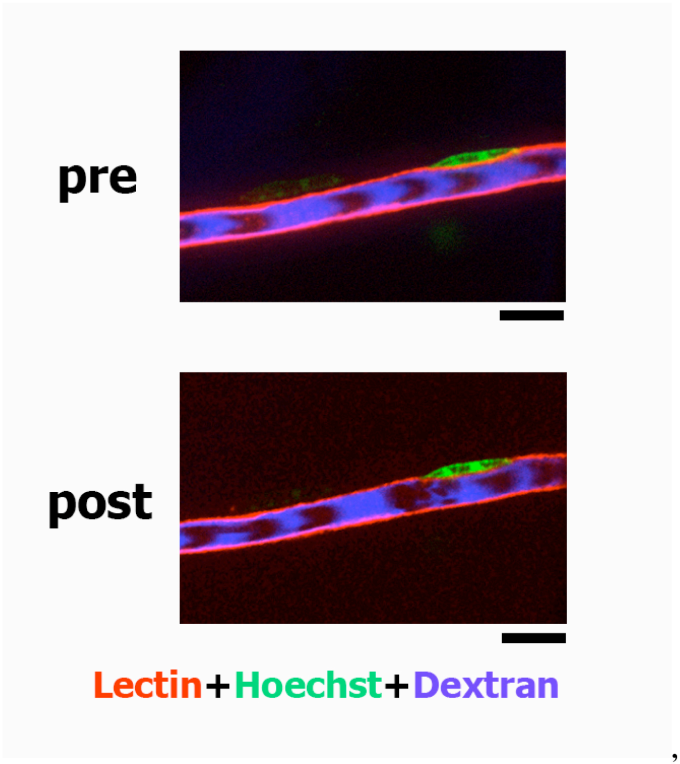

,